Wind Tunnel Determination of the Lateral-Directional Stability Derivatives of the F/A-18 E Airplane

CDR Robert J. Niewoehner, USN

August 22, 2001

Abstract

The lateral-directional stability derivatives of the F/A-18 E airplane where determined in the United States Naval Academy's 44×48 inch Eiffel Wind Tunnel using a 1/28 th scale model. Directional stability, dihedral effect and side force were all observed to behave linearly over the limited range of sideslip angles tested. As expected, the model exhibited both positive directional stability and positive dihedral. Results for the side force and dihedral derivatives were acceptable. The directional stability results were unacceptable. Redesign of the test set-up is recommended.

Contents

List of Figures

List of Tables

List of Symbols

b . . . . . wing span
C_ℓ . . . . . rolling moment coefficient (body axes)
C_{ℓ_β} . . . . . dihedral stability derivative (body axes)
C_N . . . . . nondimensional yawing moment (body axes)
C_{N_β} . . . . . directional stability derivative (body axes)
$C_{N_{\beta_{\text{balance}}}}$ . . . . . directional stability derivative(body axes/balance center)
C_Y . . . . . side force coefficient
C_{Y_β} . . . . . side force derivative
L . . . . . rolling moment (body axes)
N . . . . . yawing moment
q . . . . . dynamic pressure
x . . . . . displacement distance from balance center to model center
Y . . . . . side force

Chapter 1

Introduction

1.1 Purpose

This experiment was conducted to determine the lateral-directional stability derivatives of the F/A-18 E Super Hornet at low angles of attack and low sideslip angles.

1.2 Background and Theory

Aircraft dynamic models require determination of the aerodynamic forces and moments under a range of sideslip angles, β, and angles of attack, α. In particular, the flight control design and analysis process initially uses analytical tools to determine the expected stability characteristics of a design. As a design matures, wind tunnel studies improve the fidelity of the design models by direct measurement of the forces and moments at the flight conditions of interest. This study focused on determining the lateral and directional forces and moments produced by variations in the sideslip angle.

Figure 1.1 illustrates the industry standard sign convention. All forces and moments are reported in the body axis coordinate system. Positive sideslip is defined as nose left (wind in the right ear). Positive side force is out the right wing. Positive moments are right roll and right yaw.

The strength of the stability of an airplane is typically expressed by "stability derivatives". Direction stability, for example, is expressed as the directional restoring moment, N, per unit sideslip angle, or $(\partial N/\partial\beta)$. The nondimensional directional stability derivative, C_{N_β}, is given by

$$C_{N_\beta} \equiv \frac{\partial C_N}{\partial \beta} \tag{1.1}$$

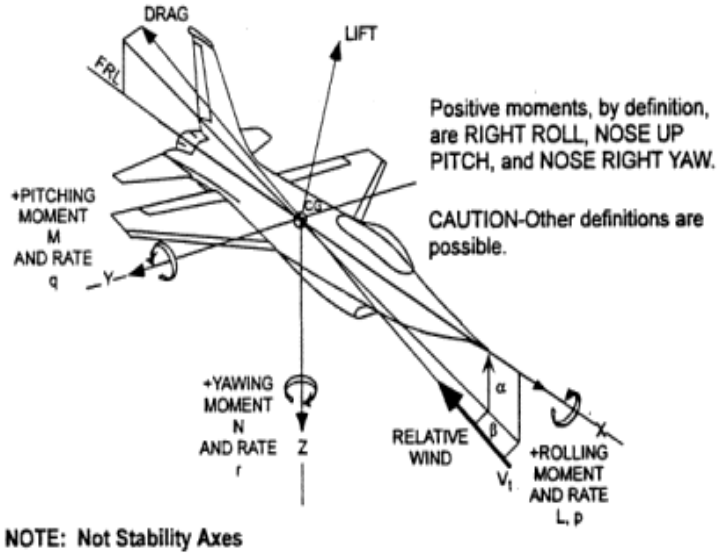

Figure 1.1: Body axis sign convention

where the moment coefficient is

$$C_N \equiv \frac{N}{qSb} \tag{1.2}$$

For positive directional stability, a positive restoring moment (nose right) is required in response to a positive (nose left) sideslip disturbance. Positive directional stability is therefore represented by positive C_{N_β}.

Dihedral effect expresses the lateral stability. Dihedral effect is the aerodynamic rolling moment (L) exerted due to sideslip and is given by

$$C_{\ell_\beta} \equiv \frac{\partial C_\ell}{\partial \beta} \tag{1.3}$$

where the rolling moment coefficient is

$$C_\ell \equiv \frac{L}{qSb} \tag{1.4}$$

For positive dihedral, a negative (left) rolling moment is required in response to a positive (nose left) sideslip disturbance. Positive directional stability is therefore represented by C_{ℓ_β}. (Caution: opportunity exists for

confusion with the two-dimensional lift coefficient, also signified by C_ℓ. The ambiguity is resolved exclusively by context.)

Side force, Y, arises from the aerodynamic force of the fuselage and vertical tail exposed to sideslip. The derivative, which is always negative, is expressed by

$$C_{Y_\beta} \equiv \frac{\partial C_Y}{\partial \beta} \tag{1.5}$$

where the side force coefficient is

$$C_Y \equiv \frac{Y}{qSb} \tag{1.6}$$

All of the above moments and forces are expected to behave linearly for small sideslip angles. The stability derivatives are therefore expected to be constants.

1.3 Test Article and Test Equipment

1.3.1 Model Description

This study used a 1/28 th scale model of the F/A-18 E Super Hornet, a twin-engine, single-place carrier-based strike fighter (see Figure 1.2). The model was representative of the mold line of the production airplane, with the exceptions listed below. The model's configuration was gear up, flaps up, with no external pylons or stores. The leading and trailing edge devices were adjustable, but were locked in their full up position with the seams taped to prevent leakage. The stabilators were adjustable, but were locked at zero degrees deflection. External antennas, carriage hardware and flap actuator fairings were not modeled. The engine inlet provided for direct, unobstructed flow through to the exhaust. The model was mounted to the sting balance between the two engine exhausts at its extreme aft end. The model center (25% mean aerodynamic chord) was located 15.96 inches forward of the balance center.

1.3.2 Wind Tunnel Description

The Eiffel Tunnel at the United States Naval Academy provides a 44×48 inch test section, with a maximum rated velocity of 16 inches of Hg (240 feet per second, or 140 knots). The tunnel is a single-pass design, open to the laboratory facility at both ends. It is equipped with both a six-component sting balance and a pyramidal balance. A wall manometer, with taps in both the settling chamber and the test section, provides test section velocity.

Figure 1.2: F/A-18 E test model

1.3.3 Instrumentation

A six-component sting balance electrically measured lift, drag and side-force loads, as well as the three moments about balance center. The automated data acquisition system sampled each component ten times per second over ten seconds, recording the sample average and standard distribution.

1.4 Scope of Test

The test evaluated the six component forces and moments at angles of attack and sideslip angles for which linear variations are expected. Test conditions are summarized in Table 1.1. The 4.2 degree angle-of-attack condition represented the value for maximum range.

1.5 Method of Test

The model was mounted on the tunnel's sting balance. A hand scale was used to confirm the calibration. The sting was electronically adjusted via the data acquisition software through the desired range of test conditions.

All data were electronically recorded and then transferred to a spreadsheet for post-processing using Excel.

Determination of the directional stability required transfer of the moment from the balance center to the model center, a distance of $x = 15.96$ inches, using the balance-centered moment and side force derivatives, i.e.

$$C_{N_{\beta_{\text{model}}}} \equiv C_{N_{\beta_{\text{balance}}}} - \frac{x}{b} C_Y \tag{1.7}$$

This approach was required due to the very small relative magnitude of $C_{N_{\beta_{\text{model}}}}$ compared to that of $C_{N_{\beta_{\text{balance}}}}$.

Table 1.1: Test conditions

Tunnel Speed	12 inches Hg
Angle of Attack	0, 4.2, 10 degrees
Angle of Sideslip	-5 to 5 degrees (1 degree increments)

Chapter 2

Results and Discussion

2.1 Side force Derivatives

Side force was evaluated at 0, 4.2 and 10 degrees angle of attack for the range of sideslip angles from -5 to $+5$ degrees. Data and a linear fit to each data set are shown in Figure 2.1, and the side force derivatives are summarized in Table 2.1. The side force derivatives varied from -0.011 at 0 degrees to -0.126 at 10 degrees angle of attack, with 95% confidence band of no more than 8%. The data exhibits strong linearity consistent with expectations, and the side force derivatives increased slightly in strength as the angle of attack increased. The confidence bands are sufficiently tight to consider the data accurate for flight control design purposes.

2.1.1 Dihedral Effect

General

The strength of the dihedral effect (rolling moment due to sideslip) was evaluated over the range of sideslip angles from -5 to $+5$ degrees. Data

Table 2.1: Side force derivatives

Angle of Attack (deg)	C_{Y_β}	95% Confidence Bound on C_{Y_β}
0	-0.0110	0.0009
4.2	-0.0118	0.0006
10	-0.0126	0.0004

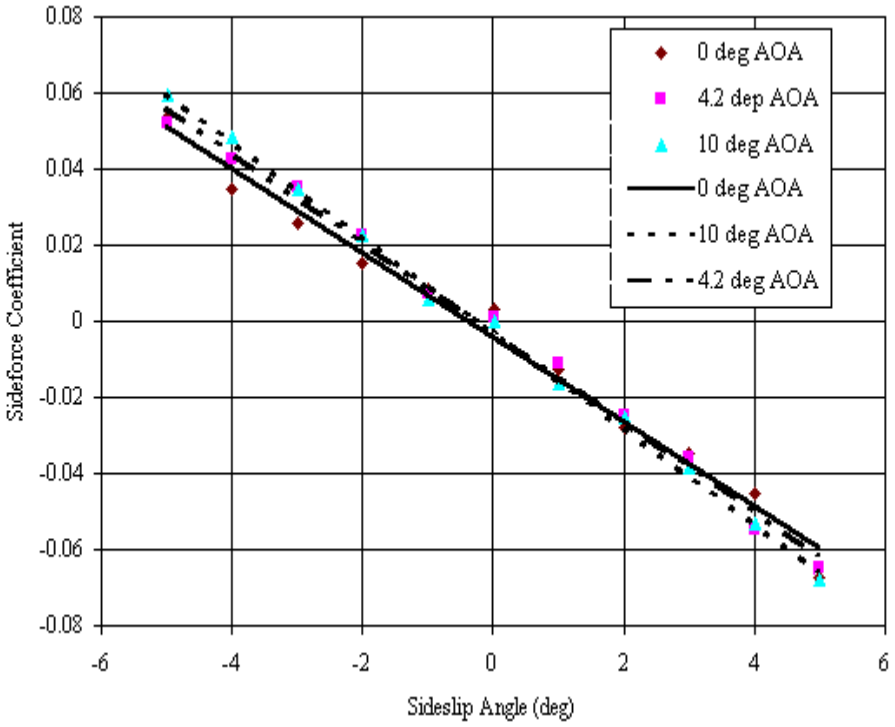

Figure 2.1: Side force coefficients

are shown in Figures 2.2 and 2.3 for 0, 4.2 and 10 degrees angle of attack, respectively. The data in Figure 2.2 shows a roll bias at zero degrees sideslip, which was later traced to drift in one of the stabilators from its trim position. Figure 2.3 shows the same data with the constant roll bias removed for each of the three angles of attack. Table 2.2 summarizes the stability derivatives. Removal of the constant roll bias had no effect on the stability derivatives.

The data exhibited strong linearity across the sideslip range, with confidence bounds of 10% or less. The data may be accepted as accurate. If tighter confidence bounds are desired, the test should be repeated with the stabilator position fixed to eliminate the roll bias.

Variation with Angle of Attack

As shown in Figure 2.3 and Table 2.2, the dihedral effect increased significantly with the increase in angle of attack and lift coefficient. Because the

Table 2.2: Corrected rolling moment

Angle of Attack (deg)	Lift Coefficient	C_{ℓ_β}	95% Confidence Bound on C_{ℓ_β}
0	0.05	−0.00068	0.00006
4.2	0.32	−0.00135	0.00007
10	0.77	−0.00171	0.00005

wing is mid-mounted on the fuselage and has no physical dihedral, variations on the lift from the upwind/downwind wing would be expected to dominate the dihedral effect. The observed variation is consequently consistent with expectations.

2.2 Directional Stability

The directional stability was evaluated at 0, 4.2 and 10 degrees angle-of-attack for the range of sideslip angles from 5 to +5 degrees. The yawing moments, as measured from the balance center, are shown in Figure 2.4.

The yawing moment coefficients about the model center were determined using Equation 1.7, and are given in Table 2.3, along with the constituent terms. Because C_{N_β} was determined as the difference of two terms of similar magnitude, its magnitude was smaller and very susceptible to the uncertainty in the other terms of Equation 1.7. Though the values of C_{N_β} were positive, indicating positive directional stability, the uncertainties for each of the calculated values were excessive and undermined their credibility. The directional stability results are not accepted as accurate. The test equipment should be redesigned to directly measure the yawing moment at the model center.

Table 2.3: Yawing moment

Angle of Attack (deg)	$C_{N_{\beta_{textrmtinybalance}}}$	$\frac{x}{b}C_{Y_\beta}$	C_{N_β}	95% Confidence Bound on C_{ℓ_β}
0	−0.00875	−0.00918	0.00043	0.00073
4.2	−0.00916	−0.00981	0.00065	0.00053
10	−0.00973	−0.001046	0.00073	0.00034

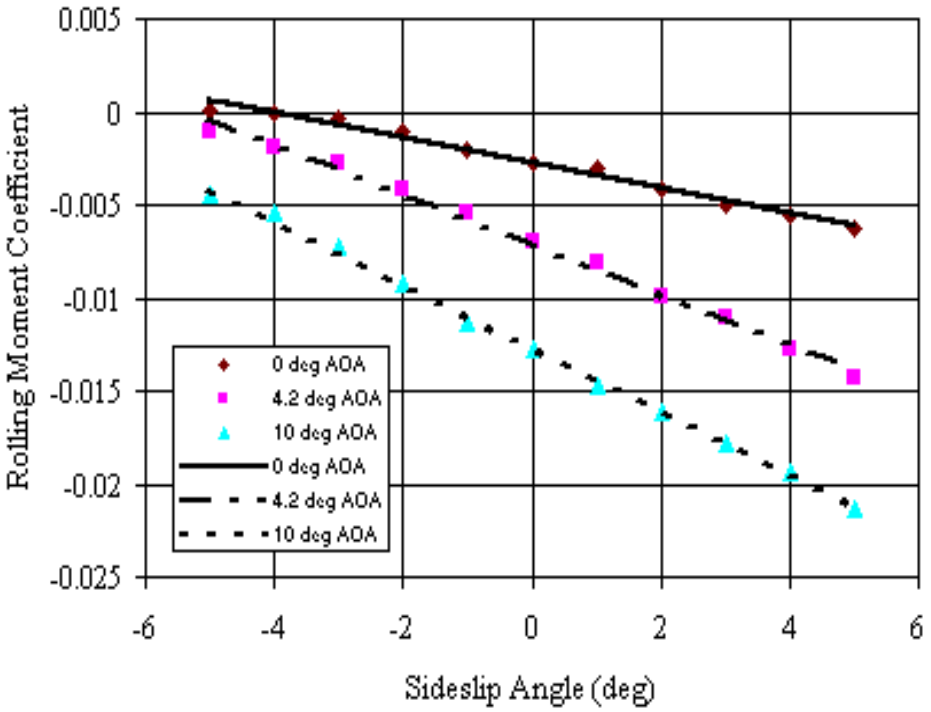

Figure 2.2: Rolling moment variation with sideslip

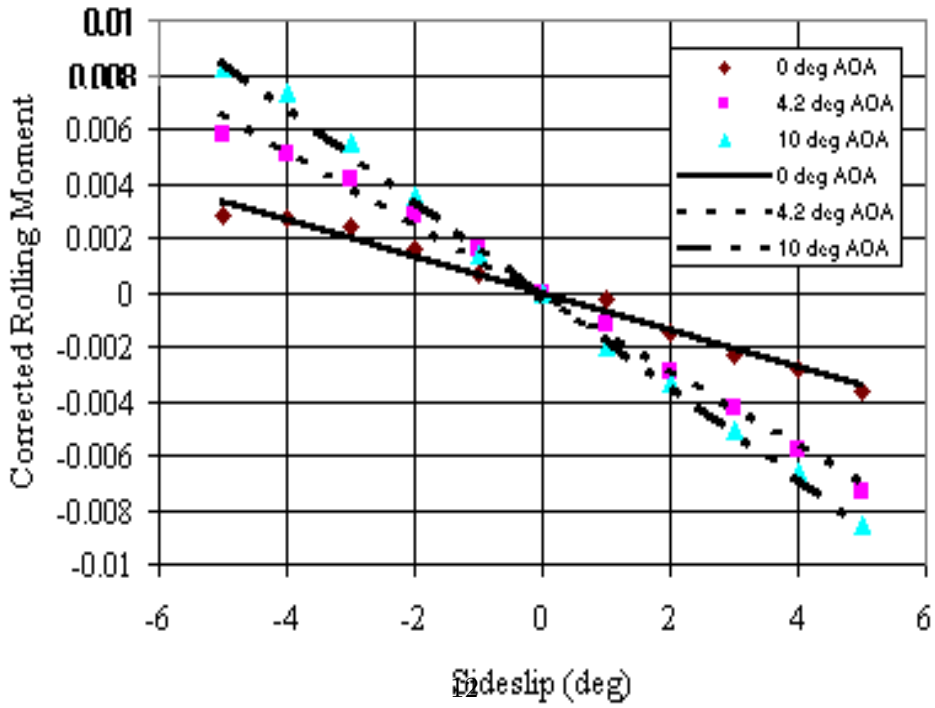

Figure 2.3: Corrected rolling moment

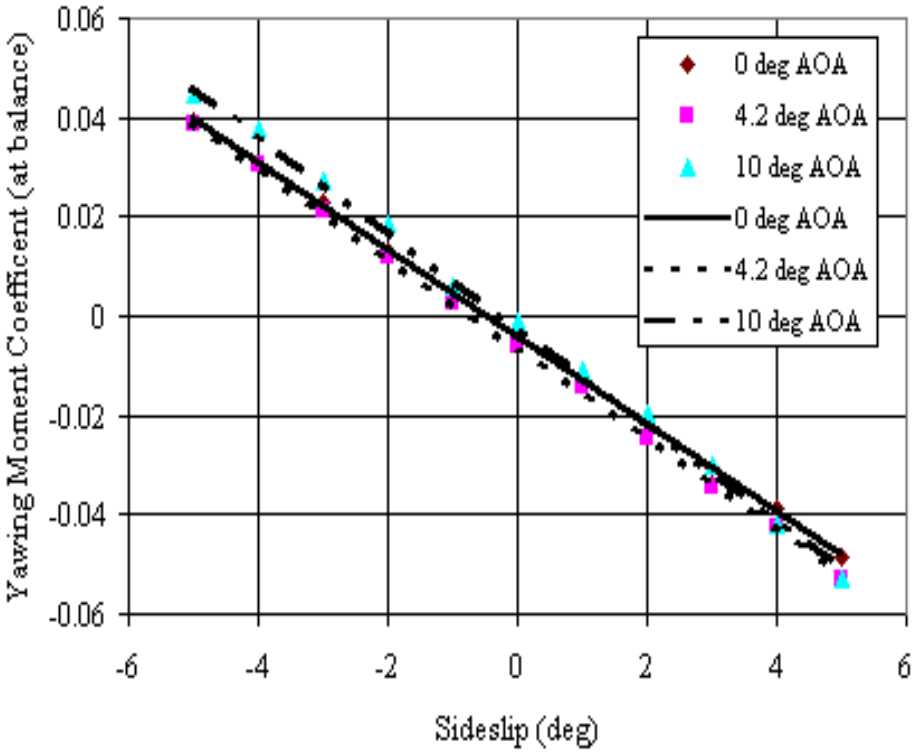

Figure 2.4: Yawing moment

Chapter 3

Conclusions and Recommendations

3.1 Conclusions

The lateral directional derivatives of the F/A-18 E airplane were determined using a 1/28 th scale model in the USNA Eiffel wind tunnel. Specific conclusions are:

a. The side force and dihedral stability derivatives exhibit trends consistent with expectations. They were determined with sufficient confidence for flight control design purposes.

b. The airplane exhibited positive directional stability; however, the directional stability results are accepted as accurate.

3.2 Recommendations

Due to uncertainties in the yawing moment measurements, the test equipment should be redesigned to directly measure the yawing moment at the model center.

3.3 References

Rogers, D.F., *EA303 Experiment 7: Student Wind Tunnel Experiments*, November, 1999.

Appendix A

F/A-18 E Wind Tunnel Model

Model Scale:	1/28	Tunnel Size:	40x44
Leading Edge Flap:	Up	Tunnel Speed:	12" Hg
Trailing Edge Flap:	Up	Sideslip Range:	-5 to +5 deg
Reference Area:	0.64 ft^2	Total Pressure:	30.37" Hg
Reference Span:	19.2 in^2		

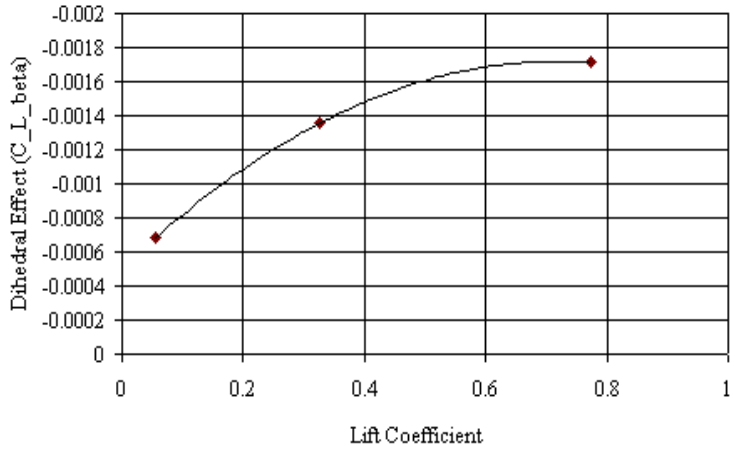

Figure A.1: Dihedral variation vs. lift